

1

COMPONENT PART NOTICE

THIS PAPER IS A COMPONENT PART OF THE FOLLOWING COMPILATION REPORT:

TITLE: Terrestrial Propagation Characteristics in Modern Systems of Communications,
Surveillance, Guidance and Control, Proceedings of the Electromagnetic Wave
Propagation Panel Specialists' Meeting Held in Ottawa (Canada) on 20-24 October 1986.

TO ORDER THE COMPLETE COMPILATION REPORT, USE AD-A194 686.

THE COMPONENT PART IS PROVIDED HERE TO ALLOW USERS ACCESS TO INDIVIDUALLY AUTHORED SECTIONS OF PROCEEDING, ANNALS, SYMPOSIA, ETC. HOWEVER, THE COMPONENT SHOULD BE CONSIDERED WITHIN THE CONTEXT OF THE OVERALL COMPILATION REPORT AND NOT AS A STAND-ALONE TECHNICAL REPORT.

THE FOLLOWING COMPONENT PART NUMBERS COMPRISE THE COMPILATION REPORT:

AD#: AD-P005 731 thru AD#: AD-P005 749.
AD#: _____ AD#: _____
AD#: _____ AD#: _____

Accession For	
NTIS GRA&I	<input checked="checked" type="checkbox"/>
DTIC TAB	<input type="checkbox"/>
Unannounced	<input type="checkbox"/>
Justification	
By _____	
Distribution/	
Availability Codes	
Dist	Avail and/or Special
A-1	

DTIC
ELECTE
JUL 08 1988
S D

REVIEW OF RECENT DEVELOPMENTS IN EVAPORATION DUCTING ASSESSMENT

by

JUERGEN H. RICHTER
OCEAN AND ATMOSPHERIC SCIENCES DIVISION
NAVAL OCEAN SYSTEMS CENTER
SAN DIEGO, CA 92152-5000
USA

SUMMARY

Continued interest in accurately assessing and exploiting evaporation ducting effects has resulted in some recent work summarized in this paper.

Available evaporation duct height and path loss models are compared (ref 1). This includes both sensitivities of duct height values to meteorological inputs and agreements between different path loss models. The models compared are those developed by Jeske (ref 2), Hitney (ref 3), and Rotheram (ref 4). Reasonable agreement of duct height calculations and path loss values derived from the different models was obtained when applied to statistically averaged meteorological inputs. Commonly used point measurements were found inadequate for reliable evaporation duct assessment. This led to the suggestion of a new shipboard deployable sensor using a single temperature sensor for air-sea temperature measurements.

Both long time statistical duct height averages and individual data sets often contain unusually high duct heights not supported by propagation measurements. Paulus (ref 5) analyzed the meteorological conditions and found a bias in commonly used measurement techniques toward stable conditions. He proposed a correction algorithm and demonstrated its utility convincingly on a set of radiometeorological measurements.

The optimum frequency for utilization of the evaporation duct for long range surface detection appears to be in the 10-20 GHz band. This is illustrated by calculating surface detection ranges for hypothetical radars equivalent in performance parameters but operating at different frequencies (ref 6).

PREFACE

The vertical decrease of relative humidity from 100% at the air-sea boundary results in a rapid vertical decrease of the refractive index. Electromagnetic waves traveling close to the water surface may be significantly influenced by such a refractive index distribution and in extreme cases may be very efficiently ducted. This oceanic evaporation duct, which is found to some degree nearly all the time over all oceanic areas, is of particular importance for over-the-horizon, surface-to-surface radar coverage. It is an important factor in the low flying ship-to-ship missile problem. To illustrate some fundamental properties of the effect of the oceanic evaporation duct on radio propagation, two vertical distributions of the modified refractivity profile are shown in figure 1. (Modified refractivity $M = (n-1) \cdot 10^6 + h/a \cdot 10^6$; n = refractive index, h = height above the surface, a = earth's radius.) The dashed line represents no evaporation ducting while the solid line is representative of good ducting conditions. Figure 2 shows the vertical distribution of path loss for the two refractivity distributions assuming a 19-nmi, 9.6 GHz over-water propagation path with one terminal at 16 feet above the water (path loss is the ratio in dB of transmitted to received power assuming isotropic antennas). The dashed curve in figure 2 indicates a decrease of path loss (or an increase of signal) with height. The solid curve corresponding to the solid M -curve in figure 1 shows a minimum in path loss (or a maximum in received signal) at a height of about 15 feet. At this height the signal enhancement over no ducting conditions is 62 dB. Signal enhancements of such a magnitude emphasize the importance of the oceanic evaporation duct. (The solid curve in figure 2 must not be extrapolated beyond the height plotted. It will not cross the "no ducting" curve but, depending on horizon range, increase with altitude.) The presentation of figure 2 may also be used to determine antenna heights for optimum utilization of ducting conditions. For example, an antenna at a height of 64 feet would receive 11 dB less signal than an antenna at 15 feet. Nonetheless, the signal enhancement from evaporation ducting would be 30 dB for the high antenna. A fact frequently overlooked is that signal enhancements from evaporation ducting are usually encountered for all possible antenna heights on board ship.

A convenient parameter for the description of ducting conditions is "duct height" defined as the height at which the M -curve attains its minimum value. Thus, the solid curve in figure 1 has a duct height of 47 feet. In general, greater duct heights will result in higher signals. However, this duct height parameter should not be misinterpreted as a height limit above which signal enhancements cannot occur. As shown in figure 2, 30 dB signal enhancements are experienced well above the duct height.

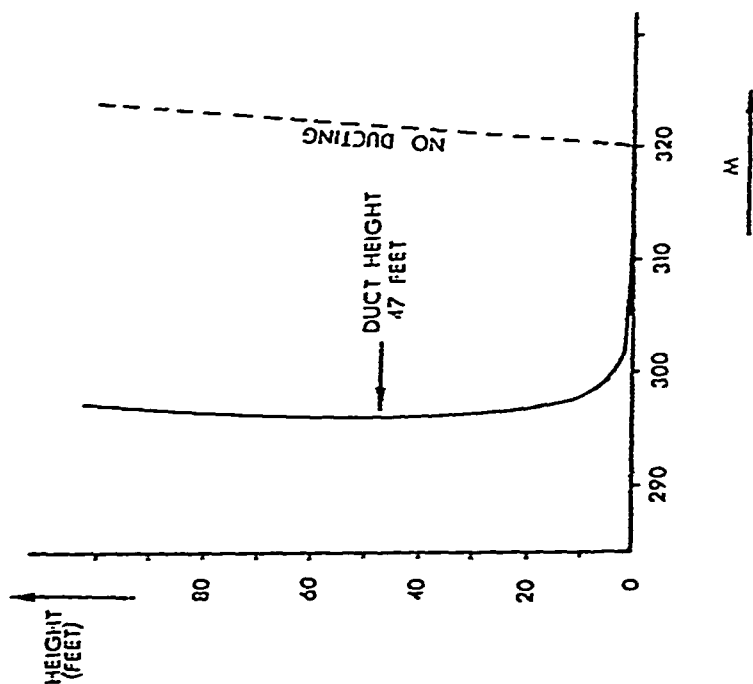


Figure 1. Modified refractivity profile M for no ducting (dashed curve) and for a 47-foot duct height (solid curve).

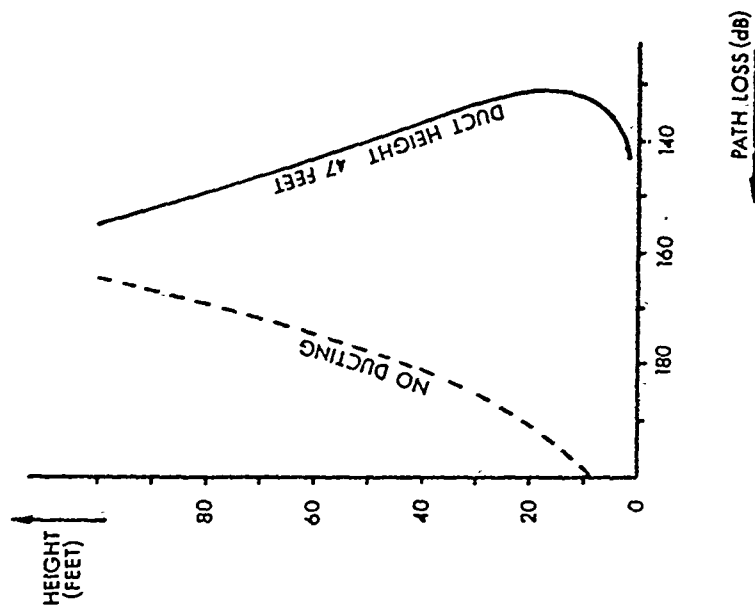


Figure 2. Path loss profiles for a 9.6 GHz, 19-rmi path with a terminal height 16 feet. The dashed curve is for no ducting and the solid curve is for a 47-foot duct height.

REFRACTIVITY PROFILES

The vertical distribution of the refractive index must be known for propagation calculations. A direct measurement of the refractive index profile under operational conditions is impractical. For instance, the profile in figure 1 changes 20 M-units within the first 4 feet above the water and only an additional 4 M-units between 4 and 47 feet. Even for moderate winds and ocean waves it would be very difficult to make measurements that close to the water surface. In addition, profiles based on single measurements usually show strong variations which often make the true profile shape unrecognizable. These variations are smoothed out only if mean values are derived by averaging over several minutes. If the functional relationship is known which governs the vertical distribution of the refractive index, then only measurements at the sea surface and at a convenient reference height are needed. Such measurements are called bulk measurements. Advances in boundary layer research have made it possible to derive profile descriptions which are adequate to describe radio propagation conditions. Those profiles are dependent on turbulent transfer processes and assume different shapes depending on the thermal structure in the boundary layer. Under thermally neutral conditions (adiabatic lapse rate) a logarithmic profile describes the vertical distribution of the meteorological parameters of interest. For non-neutral temperature conditions (diabatic lapse rate) the vertical gradient of the meteorological parameters is modified by a function which depends on stability. According to Jespersen (ref 2), in the stable region a stability function first proposed by Monin and Obukhov (ref 7) should be used which results in a logarithmic-linear profile. Under intense thermal stratifications the turbulence theories used are no longer valid. Therefore, for stabilities exceeding a bulk Richardson's number of one, no general functional relationship for the vertical distribution of the meteorological parameters is presently available. Bulk Richardson's number can be determined from the temperature difference ΔT (in K) between the surface and a reference height z_1 (in m) and the wind speed u (in knots, measured at z_1) according to

$$R_{ib} = 1.3z_1 \frac{\Delta T}{u^2} \quad (1)$$

The logarithmic-linear profile also provides the satisfactory profile descriptions in the unstable region ($R_{ib} < 0$). However, a different stability function provides more accurate profiles for superadiabatic lapse rates (ref 2). Based on the two stability functions for stable and unstable conditions duct height DH (in m) may be calculated according to the following formulas.

Stable region ($0 < R_{ib} < 1$):

$$DH = \Delta N / (b_1 B - \Delta N \alpha / L') \quad (2)$$

where

$$B = \ln(z_1/z_0) + \alpha z_1/L'$$

ΔN is the refractivity difference between surface and reference height, z_1 , b_1 is a constant with the value of -0.125 m, the hydrodynamic roughness of the sea $z_0 = 1.5 \times 10^{-3}$ m, $\alpha = 4.5$, and L' is the so-called Monin-Obukhov length. The Monin-Obukhov length can be determined from an empirical relationship between bulk Richardson's number and a so called profile coefficient (ref 2).

Unstable Region ($R_{ib} < 0$):

$$DH = [(b_1 B / \Delta N)^4 - 4\alpha (b_1 B / \Delta N)^3 / L']^{-1/4}$$

where

$$B = \ln(z_1/z_0) - \phi \quad (3)$$

The function ϕ may be found in ref 8. Further refinements of boundary layer models have been attempted based on the so-called Businger-Dyer stability function (ref 9-10).

DUCT HEIGHT NOMOGRAMS

The measurements necessary for duct height calculations according to equations (1) - (3) are surface water temperature TS and, at some convenient reference height, air temperature TA, relative humidity RH, and wind speed WS. Refractivity N is calculated from

$$N = \frac{77.6 P}{T} + \frac{3.73 \times 10^5 e}{T^2} \quad (4)$$

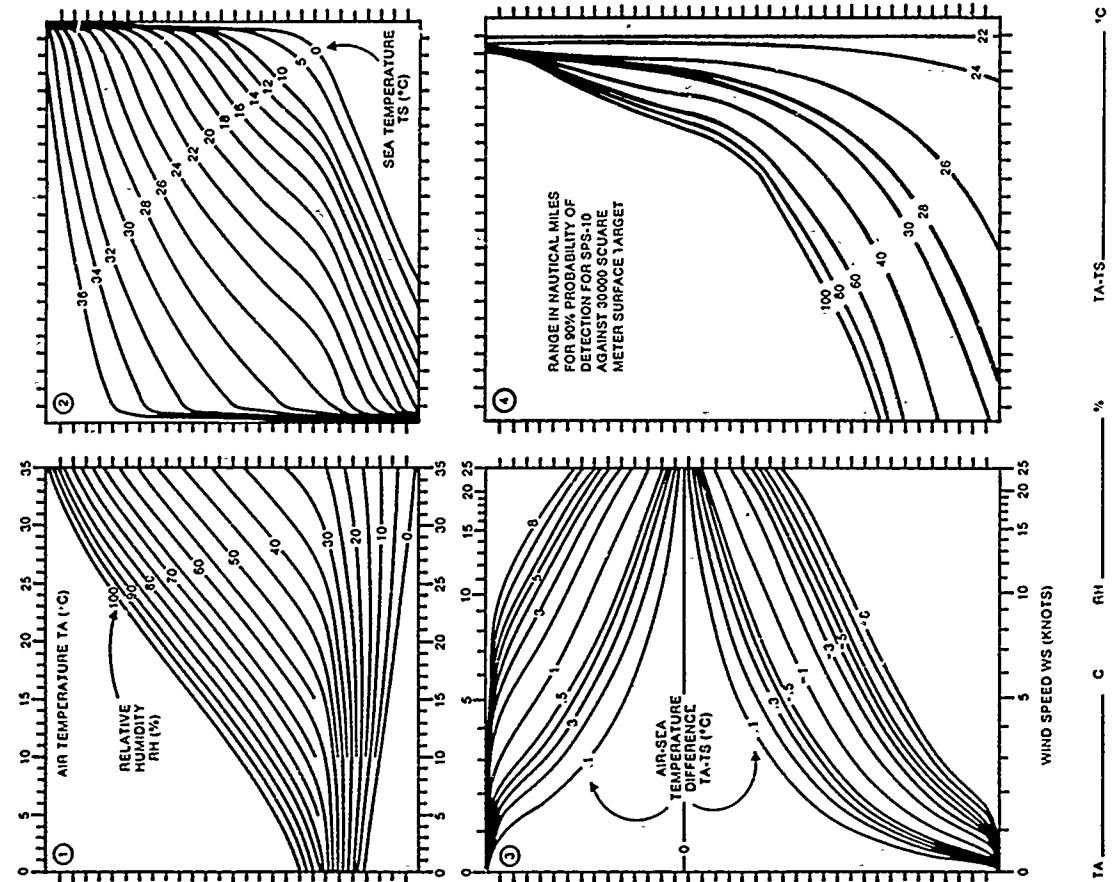


Figure 3. Evaporation duct nomogram.

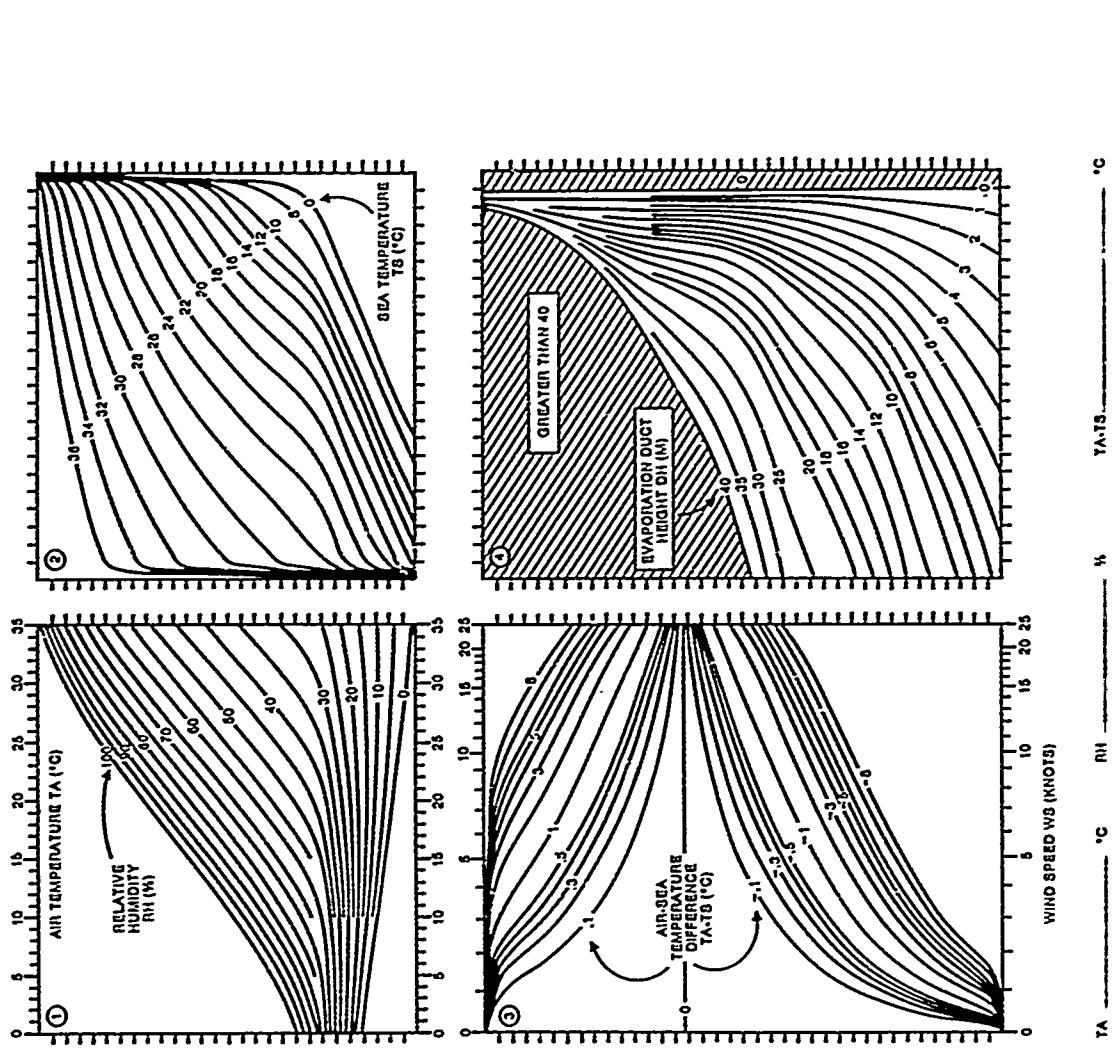


Figure 4. Detection range calculator of an SPS-10 radar against a 3000 square meter target under evaporation ducting conditions.

Where P is atmospheric pressure in millibars, T is temperature in Kelvins, and e is water vapor pressure in millibars. A simple nomogram (figure 3) was developed which provides an easy means for deriving evaporation duct height based on simple bulk meteorological measurements. Starting at graph 1 in figure 3, a horizontal line is drawn for the measured RH and TA values until it intersects the appropriate TS curve in graph 2. From this intersection a vertical line is drawn into graph 4 where the intersection with a horizontal line starting at the measured TA-TS and WS values of graph 3 gives the duct height DH. Since evaporation duct height by itself does not give quantitative systems performance data, additional nomograms have been developed in which the graph for duct height is replaced by, for instance, a radar detection range graph. In figure 4 the range of detecting a 30000 m² target with a 90% probability using an SPS-10 radar is shown (graph 4). Besides eliminating cumbersome and lengthy calculations, figures 3 and 4 illustrate also the sensitivity of evaporation ducting assessment to the measurement accuracy of the input parameters. For example, small changes to air-sea temperature differences values may significantly change duct heights and detection ranges. Both nomograms shown in figures 3 and 4 are based on models and their verification described by Hitney (ref 3) and Richter and Hitney (ref 11).

MODEL SENSITIVITIES

Patterson (ref 1) recently compared the relative performance of evaporation duct and path loss models. He found that the models performed reasonably well when considering statistically averaged meteorological inputs but, not surprisingly, were extremely sensitive to point-observed meteorological input parameters. He concluded that the measurement techniques employed by naval and transiting commercial vessels are not of sufficient quality to calculate individual evaporation duct heights. Figures 5 and 6 illustrate the spread between measured and calculated 9.624 GHz path loss data based on the models used by Rotheram (ref 4) and by the Integrated Refractive Effects Prediction System (IREPS) (ref 2, 11, 12, 13). (The measured data are from ref 11, November period, path length 19 nmi, transmitter antenna height 5 m). Since small uncertainties in air-sea temperature differences (see figure 3) may cause significant changes in duct height, an evaporation ducting sensor development program is being conducted at the Naval Ocean Systems Center, which uses a single sensor for TA and TS measurement. This eliminates the need of accurate cross calibration for different sensors. A very fast response thermistor probe, connected by wire to a shipboard processing unit, is thrown from a convenient shipboard location into water undisturbed by the moving ship. During the fall the probe measures TA and, subsequently, TS when entering the water. The probe may be retrieved or made expendable. Initial tests showed that air-sea temperature differences of 0.1 Celsius are obtainable. This, by far exceeds, commonly achievable accuracies and should improve individual evaporation duct height measurements significantly.

CORRECTION ALGORITHM

Examining evaporation ducting statistics like the one shown in figure 7 (for Marsden Square 88, Hawaii), one often finds high percentages of duct height occurrences for large duct heights (all duct heights in excess of 40 m are combined in the column 40-42 m). Such large evaporation duct heights are difficult to explain from a micrometeorological interpretation, are not supported by radio propagation observations and are not found in meteorological measurements for which special care has been taken like meteorological buoy observations (ref 5). The most likely error source is surface heating in TA measurements which leads to erroneous high thermal stabilities. Paulus (ref 5), based on a number of careful arguments, introduced a modified duct height calculation algorithm in which stable, high humidity conditions are accepted and stable, low humidity conditions are assumed to be in error and defaulted to unstable. This algorithm applied to the data of figure 7 produces a much more reasonable distribution and is shown in figure 8. Even more convincing is an application of Paulus' (ref 5) technique to 18 GHz propagation measurements over an 81 km over-water path (transmitter and receiver heights were 19 m and 11 m, respectively). The solid curve in figure 9 is the calculated path loss for this geometry and the dots are measured values. When Paulus' technique (ref 5) was applied to the measured values of figure 9, a significantly better agreement was obtained as shown in figure 10. From the evidence so far it appears that Paulus' modified duct height calculations are capable of dramatically improving evaporation ducting statistics.

SURFACE DETECTION RANGES

Based on measurements described in ref 11, it appears that signal enhancements from evaporation ducting are largest in the 10-20 GHz frequency range. For higher frequencies molecular absorption, scattering from the rough ocean surface, inhomogeneities in the evaporative duct and scattering from aerosols counteract the otherwise increased effectiveness of the wave guiding mechanism. Anderson (ref 6) compared four hypothetical radars with equivalent performance characteristics but operating at frequencies of 3, 6, 10, 18 GHz. He used a global refractivity climatology (ref 14) and propagation models discussed in ref 15 to calculate the probability of detecting surface targets at ranges well beyond the normal radar horizon. The results are displayed in figure 11 and show both a latitude dependence, i.e., the evaporation ducting effect is stronger in lower latitudes, and the superior performance for frequencies in the 10-20 GHz frequency band.

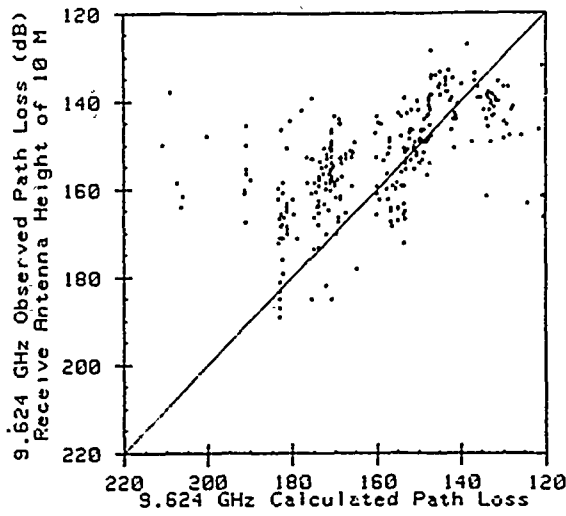


Figure 5. Observed calculated path loss for Rotheram models (ref 4).

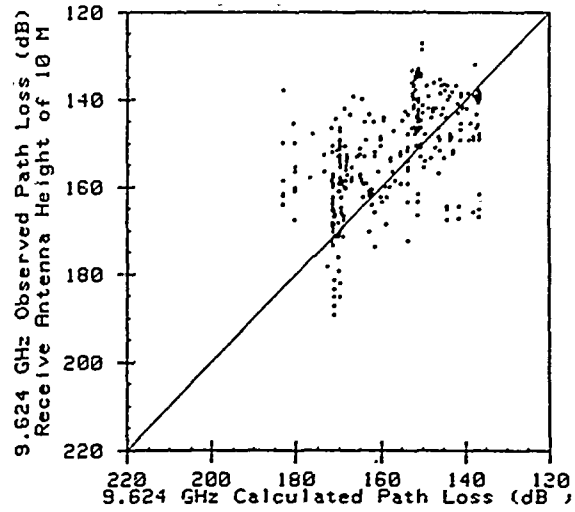


Figure 6. Observed versus calculated path loss for IREPS (ref 2, 11, 12) models.

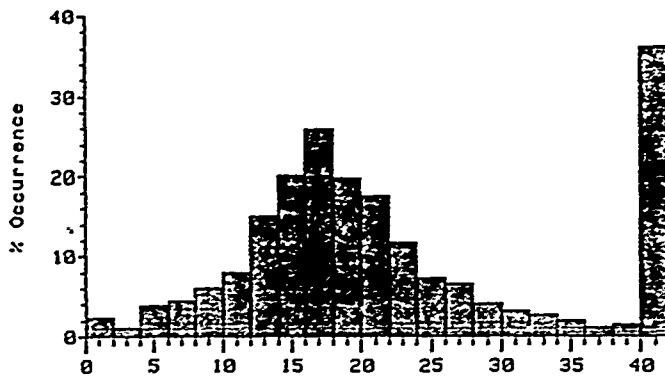


Figure 7. September IREPS duct height distribution for MS 88.

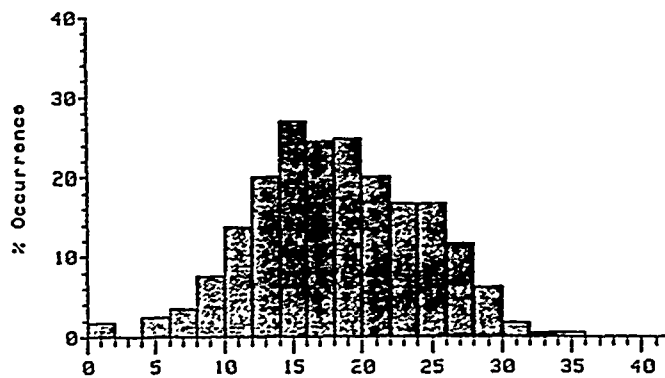


Figure 8. September modified duct height distribution for MS 88.

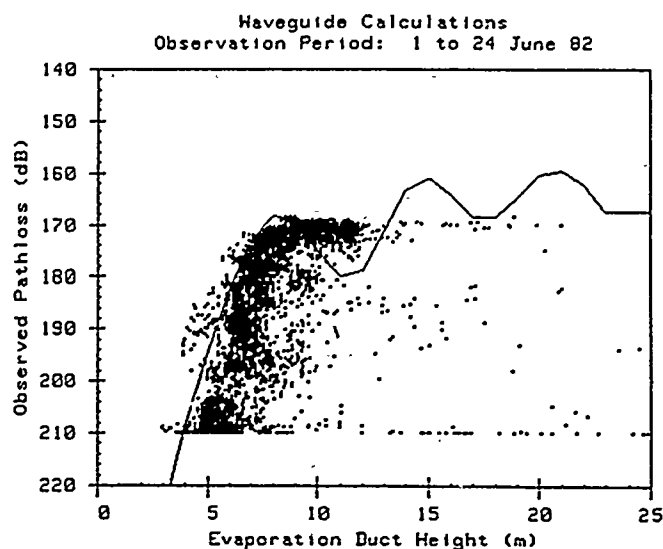


Figure 9. Comparison of experimental measurements to waveguide predictions.

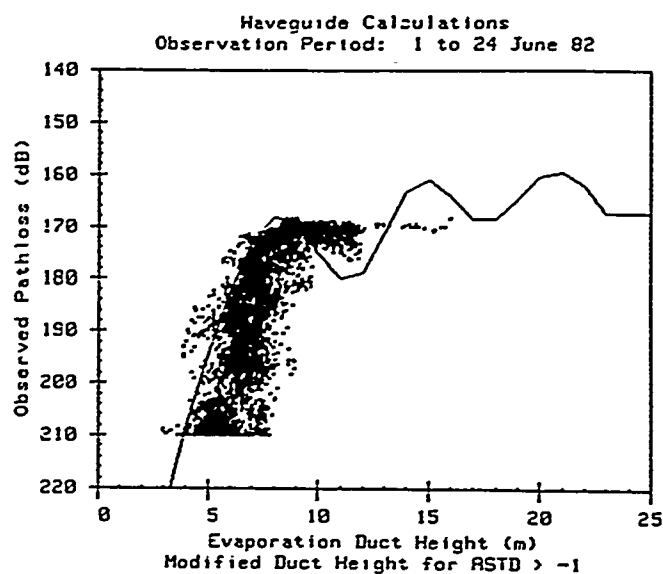


Figure 10. Comparison of experimental measurements to waveguide predictions in which all data points based on an air-sea temperature difference greater than -1°C were subjected to a modified duct height calculation.

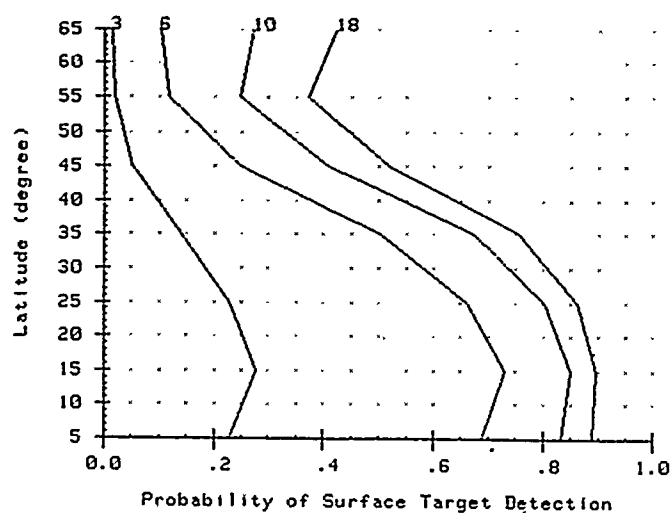


Figure 11. Geographic influence of the evaporation duct on shipboard radar surface-target detection capabilities. The target is well beyond the normal horizon and the increased detection range is solely due to the evaporation duct. Predictions are for four radar frequencies; 3, 6, 10, and 18 GHz.

CONCLUSIONS

Evaporation ducting is an important propagation enhancement mechanism over the oceans of continued scientific interest. Recent efforts have shown that presently used models appear adequate for statistical assessments. An important correction algorithm was developed to remove erroneously high duct heights. A new air-sea temperature probe is under development which is expected to improve in-situ evaporation ducting assessment. Future work should address propagation modeling under horizontally inhomogeneous conditions, investigation of sensing techniques for the three-dimensional evaporation ducting structure and development of meteorological forecasting techniques.

ACKNOWLEDGMENT

This work was supported by the Office of Naval Technology under the Atmospheric Effects on EM/EO Propagation program.

REFERENCES

1. Patterson, W.L., "Comparison of Evaporation Duct and Path Loss Models," Radio Science, 20 (5), pp 1061-1068, 1985.
2. Jeske, H., "The State of Radar Range Prediction Over Sea," AGARD Conf. Proc., 70 (2), pp 50.1-50.10, 1971.
3. Hitney, H.V., "Propagation Modeling in the Evaporation Duct," Naval Electronics Laboratory Center TR 1947, 1975.
4. Rotheram, S., "Radiowave Range Prediction Over the Sea in Evaporation Ducting Conditions," Marconi Research Laboratory, TR 77/37, 1977.
5. Paulus, R.A., "Practical Application of an Evaporation Duct Model," Radio Science, 20 (4), pp 887-896, 1985.
6. Anderson, K.D., "Surface-Search Radar Performance in the Evaporation Duct: Global Predictions," Naval Ocean Systems Center TR 923, Rev A, 1983.
7. Monin, A.S. and A.M. Obukhov, "Basic Laws of Turbulent Mixing in the Ground Layer of the Atmosphere," Akad. Nauk. USSR Geofiz. Inst. Tr., (151), pp 163-187, 1954.
8. Lunley, J.L., and H.A. Panofsky, "The Structure of Atmospheric Turbulence," New York, Interscience Publishers, 1964.
9. Businger J.S., J.C. Wyngaard, Y. Izumi, and E.F. Bradley, "Flux-profile Relationships in the Atmospheric Surface Layer," J. Atm. Sci., (28), pp 181-189, March 1971.
10. Rotheram, S., "Radio Propagation in the Evaporation Duct," the Marconi Review, XXXVII, No. 192, pp 18-40, 1974.
11. Richter, J.H. and H.V. Hitney, "The Effect of the Evaporation Duct on Microwave Propagation," Naval Electronics Laboratory Center, TR 1949, 1975.
12. Hattan, C.P., "Propagation Models for IREPS Revision 2.0," Naval Ocean Systems Center, TR 771, 1982.
13. Hitney, H.V. and J.H. Richter, "Integrated Refractive Effects Prediction System," Nav. Eng. J. 88 (2), pp 257-262, 1976.
14. Patterson, W.L., "Climatology of Marine Atmospheric Effects," Naval Ocean Systems Center, TD 573, 1982.
15. Hitney, H.V., J.H. Richter, R.A. Pappert, K.D. Anderson, and G.B. Baumgartner, "Tropospheric Radio Propagation Assessment," Proc. IEEE 73 (2) pp 265-283, 1985.

DISCUSSION

E.Vilar

- (1) You presented results obtained in the early 70s at several frequencies, X-band in particular, between two Greek islands. Could you tell us the transhorizon path length?
- (2) We are currently concerned in Europe with transhorizon interference over-sea paths (part of Eurocop COST 210). Could you please comment about the desirability and minimum sample of meteorological data to correlate our observations with the existence of an evaporation duct?

Author's Reply

- (1) Path length was 19 nmi with terminal heights of 5 m (see figure 16 of reference 15).
- (2) The parameters describing the evaporation duct must be carefully measured as described in the preceding paper. In addition, upper air soundings should be taken to differentiate between ground-based ducting effects caused by elevated refractive layers and evaporation ducting effects.

L.B.Felsen

Because the physical environment presents a multiparameter problem, where the parameters themselves are not well defined, no progress can be made on analytical and numerical modelling unless some sort of error bars can be put on the parameters. Those tolerances then can guide the modeller as to whether attempts at improving presently available predictive algorithms are likely to bear fruit. Do you feel that more can or *must* be done to sharpen the question, or have we reached an impasse?

Author's Reply

More can and must be done in providing experimental data to validate existing models and guide the development of new ones. The problem in obtaining good experimental data is cost and time. Measurement of all relevant physical parameters is expensive and encountering a sufficient large range of the uncontrolled variables may require long measurement periods or many repetitions. Once acquired and properly documented, good experimental data can and have been used for many decades in various model validation purposes.

H.Vissinga

Can you elaborate somewhat on the physics of the evaporation duct in the presence of a rough sea surface. In view of the fact that duct height and wave height are not that different in magnitude can an evaporation duct exist over a rough sea?

Author's Reply

As one can see from figure 3, duct height increases with increasing surface winds under unstable conditions. Since surface winds are directly related to sea surface roughness, one would not expect the simultaneous occurrence of rough seas and small duct heights. Extremely high winds will create a well mixed atmosphere with no evaporation duct. In our measurements, sea surface roughness affected path loss values only for frequencies well above X-band.

